



Multi-roll levelling method for longitudinal waves in metal sheet based on a coupled curvature integration model

Guodong Yi¹ · Ye Gu¹ · Lemiao Qiu¹ · Chao Wang¹

Received: 2 June 2019 / Accepted: 4 November 2019 / Published online: 2 January 2020
© Springer-Verlag London Ltd., part of Springer Nature 2020

Abstract

Longitudinal waves are the main flatness defects of metal sheets. This defect is typically eliminated by repeated elastoplastic bending via a multi-roll leveller to make the residual curvature of the sheet as small as possible. Therefore, an effective mathematical model is important for the leveller design and levelling parameter adjustment. In this paper, based on the basic principle of multi-roll levelling for the longitudinal wave of a metal sheet, a geometric model of multi-roll levelling was established via the curvature integration method; a bending-moment curvature model was also established to account for the residual curvature of reverse bending and the difference between the elastic section and the elastoplastic section. A coupled curvature integration model was constructed by combining the two models to systematically describe the multi-roll levelling process, and the variation of the curvature, surface profile curve and plastic deformation rate of the sheet during levelling were discussed; the influence of the intermesh of the work rolls on the levelling effect of the longitudinal wave was analysed. The results show that there are infinite intermesh combinations of the first work roll and the last work roll that make the residual curvature of the sheet close to zero after levelling. The results also show that the residual curvature is much more sensitive to the variation of the first work roll than to the variation of the last work roll.

Keywords Multi-roll levelling · Flatness defects · Longitudinal wave · Metal sheet · Coupled curvature integration model · Elastoplastic bending deformation · Residual curvature

1 Introduction

Flatness defects typically appear after the rolling of metal sheets due to transverse nonuniformity of the longitudinal strain; the defects include buckling or waviness (centre waves, wavy edges, quarter buckles, etc.), with longitudinal waviness being one of the most significant defects. The geometric characteristics of the defects, in the form of the height and length of the waves, are used as a measure of the geometrical quality of the rolled sheets [1–5]. The multi-roll leveller is used to eliminate longitudinal waves by applying a gradually decreasing elastoplastic deformation to the sheet so that the residual curvature of the sheet is as small as possible after levelling. The residual stress distribution after levelling is of great

importance. While a strip might be flat, the residual stress distribution will be disadvantageous during further processing. If the main parameters of the multi-roll leveller, such as levelling force and levelling power, are set improperly, then the residual stress distribution may be problematic and may lead to flatness defects downstream in the production process. Therefore, it is important to carefully analyse the longitudinal wave levelling mechanism and establish a mathematical model to calculate the effect of residual stress on the final shape of the metal sheet [3, 6–13].

Analytical, numerical and experimental methods are used to study the levelling process of the metal sheets [14].

First, the analytical methods are reviewed. Doege et al. developed an analytical forming model to investigate the state of multiple forming under bending conditions and calculate the residual stresses and the residual bend of sheet metal during the levelling process [6]. Behrens et al. developed an analytical 3D simulation to investigate the effect of the levelling process on sheet metal and calculate the remaining shape defects after levelling [15]. Nakhoul et al. proposed a two-scale model based on the generalized continuum approach to

✉ Lemiao Qiu
qiulm@zju.edu.cn

¹ State Key Laboratory of Fluid Power & Mechatronic Systems, Zhejiang University, Hangzhou 310027, China

determine the occurrence and geometric characteristics of on-line manifested flatness defects [5]. Chen and Brauneis et al. proposed a 2.5D analytical approach for the levelling process of steel plates using three steps: first, the plate is divided into several independent longitudinal strips; then, the shape and levelling forces of each strip are determined by solving the 1D beam bending problem and finally, the forces resulting from all strips are combined to obtain a discrete distribution of forces [16, 17]. Feng et al. developed an advanced 3D mathematical model for the cold rolling strip process that uses the multi-slab strategy to deal with the differential reduction in the transverse direction due to roll deformation and uses analytical solutions of roll-bending and flattening, which are discretized using the influence function method [18].

Second, the numerical methods are reviewed. Abdelkhalek et al. applied a steady-state elastic-viscoplastic finite element model to predict strip flatness and out-of-bite buckling during the cold rolling of thin strips [19]. Weiss et al. analysed the rolling process using finite element analysis, determined the distribution of residual stresses to obtain theoretical moment curvature characteristics, and qualitatively demonstrated how the material is softened in bending due to residual stress gradients after rolling [20]. Traub et al. presented a numerical modelling approach that combined global- and sub-models, enabling a high-resolution calculation of the strain distribution at acceptable computational costs without significantly delaying the planning process [21]. Mathieu et al. introduced a numerical model for a strip passing through a simplified industrial leveller (composed of four rolls), which includes shell element discretization and frictional contact between the strip and rolls, to predict the final strip shape based on the plastic strains and residual stresses occurring through the width and thickness of the strip [22]. Wang et al. developed the multi-pass roll forming control algorithm based on the actual roll-bending data. They analysed the influence of rolling bends on the forming quality of the sheet by numerical simulation [11]. Grüber et al. proposed a numerical model with three individual load triangles that evaluated the correlations between the incoming strip condition, the roll intermeshes and the residual stresses to achieve both a constant flatness and a distinct residual stress distribution after levelling [13].

Third, the experimental methods are reviewed. Weiss et al. tested strips by rolling them in tension and pure bending in a laboratory mill to investigate the material behaviour when operating close to the elastic-plastic transition point by introducing residual stresses into the material [20]. Tran et al. proposed an experimental setup to analyse the interaction between residual stress and buckling in producing wavy edge flatness defects, focusing on the influence of surface imperfections and global tension on the wrinkling characteristics [8, 12]. Abvabi et al. presented a method to determine the residual stress distribution in the sheet material from the data collected

in a free-bending test, which provides a good fit to the finite element analysis of bending when using an experimentally derived moment-curvature relation [9]. Stadler et al. investigated the control of the curvature and contact force at the strip-roll contact point of a metal strip using an experimental device and derived a material model and a steady state strip deformation model to compute feasible combinations of curvature and contact force [23].

Typically, analytical methods analyse the levelling process with sufficient precision and over a shorter duration than is possible with numerical methods [6, 24, 25]. However, numerical methods are increasingly applied in industry due to the advantage of reducing design iterations by allowing the designer to investigate the effects of parameter changes without expensive tooling costs [26].

Considering the advantages of different methods, improved models and comprehensive models have been proposed. Abdelkhalek et al. presented a predictive model of the flatness defects of thin plates during rolling using a coupled approach of simple buckling criterion and an FEM (finite element method) model of strip and roll deformation, with the model being primarily devoted to cases where on-line (under tension) defects occur [2, 27]. Dratz et al. developed three different models to determine the loading modes experienced by the material in roll levelling operations (a finite element approach, an analytical model and a semi-analytical model) and found that the semi-analytical model is the most appropriate for determining the parameters of roll levellers; the analytical model is sufficient for defining the size of the levellers [28]. Silvestre et al. developed the following analytical model and a finite element model to analyse roll levelling operations: the one-dimensional, analytical levelling model is based on classical beam theory and is used to calculate the induced strain distribution through the strip and, hence, the evolving elastic/plastic stress distribution; the 2D modelling is used to investigate differing settings, leveller configurations and materials based on assumed planar strain conditions [14]. Lee et al. proposed a simple and effective method for designing the levelling process using a combination of an analytical model and finite element analysis, as follows: the bending-moment curvature relationship is determined using finite element analysis of uniform bending using simulation results, and the proper roll arrangement corresponding to optimal curvature is calculated using the analytical model based on the curvature integration method [29]. Nakhoul coupled a simple buckling model to a finite element rolling model to solve practical problems concerning flatness in cold strip rolling and investigated the effect of residual stress on the defects in very thin strips [30]. Yu et al. adapted graphic method and mathematical induction to analyse the deformation process of the section of bar, and established the quantitative analysis model and finite element model of the two-roller straightening process [10]. Traub et al. presented a numerical modelling approach that combined

global- and sub-models to enable a high-resolution calculation of the strain distribution in the bending zone at acceptable computational costs, which is a feasible approach for providing detailed information about the strain distribution [21]. Galkina et al. proposed a model-based predictive approach for steel strip motion in hot rolling finishing mills based on a simplified nonlinear mathematical model, which was generated in the form of ordinary differential equations, and an FEM model of the strip and the roll gap [31]. Laugwitz et al. presented a closed-loop, controlled finite element model; this model couples the information obtained by multiple different simulations with the results from an on-line flatness gauge to establish an appropriate levelling strategy that can eliminate incoming flatness defects and evaluate the required set of roll positions within a single pass [32].

Calculation methods for the parameters of the leveller were also proposed. Baumgart presented a mathematical deflection model of the work rolls and the machine frame of a hot leveller; the model calculates the roll gap along both planar directions of the plate, and machine frames are modelled by linear force-deflection relations to analyse the influence of the various adjustment and control inputs on the roll gap, which is important for the levelling result [33]. Nakhoul et al. studied the impact of friction and strip tension on the flatness of a rolled thin strip, and the study showed that the optimal setting of the work roll bending force should be changed when friction varies [34]. Liu et al. built an optimization model with equality and inequality constraints to express the typical ranges of the levelling capacity by using several boundary curves that determine if an incoming plate can be levelled quickly; these curves can be used to find the maximum yield stress for a specific thickness or the maximum thickness for a given yield stress [35]. Brauneis et al. presented a mathematical deflection model of a leveller for cold, heavy plates and calculated the work roll profile, the levelling forces for a given plate, the adjustment of the leveller, and the unknown displacements of the work rolls by combining the force-deflection relations of the machine model with a nonlinear plate model [36]. Stadler et al. derived a material model and a steady-state strip deformation model based on curvature control and the contact force at the strip-roll contact point in an experimental device, and computed feasible combinations of curvature and contact force [23]. Brauneis presented a fast and robust mathematical model for the levelling process of steel plates, calculated the levelling forces for a given plate and leveller work roll configuration, and validated the model with measurements from an industrial leveller [17].

The curvature integration method is worth noting here. Liu et al. developed a mechanics model based on the curvature integration method that utilizes a nonlinear, unconstrained global optimization method to predict the plate levelling process. The study shows that the model gives results closer to experimental data than the other models [7]. Cui et al. applied

the curvature integration of elastic-plastic differences to analyse the effect of levelling strategies on the quality of plate products and to simulate the levelling results by using a different levelling strategy. The analysis proved to be an effective solution to the levelling problem [37, 38].

Multi-roll levelling is a process of repeated sheet bending, and the previous bending state will affect the subsequent reverse bending. However, only the geometric coupling relationship of the sheets between the work rolls is considered in the present curvature integration methods. The curvature coupling, that is, the influence of the residual curvature of the previous bending on the subsequent bending, is not considered when establishing the bending moment model. Moreover, this method does not distinguish between the different curvature properties of the elastic section and the elastic-plastic section of the sheet. Therefore, it is difficult to ensure the accuracy of multi-roll levelling in respect to longitudinal waves.

This paper studies the multi-roll levelling method for longitudinal wave defects in metal sheets. The bending-moment curvature model, which is based on the geometric curvature integration model, considers both curvature coupling and the difference between the elastic and elastoplastic sections. The coupled curvature integration model is constructed by combining the two models. For a metal sheet with given initial residual curvature, the relationships between the intermesh values of the first roll and last roll and the residual curvature after levelling are established. The variation of key parameters, such as curvature, plastic deformation rate and surface profile curve in the multi-roll levelling process, are discussed.

2 Coupled curvature integration model

There are three problems that must be considered when establishing a multi-roll levelling model for longitudinal waves in a metal sheet, as follows: first, the complex coupling relationships between adjacent sections of the sheet that are divided by the work rolls must be evaluated; second, the boundaries between the elastic deformation sections and the elastoplastic deformation sections of the sheet must be assessed; and third, the actual contact positions of the sheet and the work rolls in the levelling process must be determined.

Meanwhile, the curvature integration mathematical model is based on the following assumptions: (1) The only forces applied to the sheet during levelling are the shearing forces of the work rolls, in which tension forces and friction between the roll and sheet are neglected; (2) Work hardening of the sheet is neglected, which is used in the multi-roll levelling a sheet metal with low enhancement coefficient; (3) The bending moments on the sheet of the first and last roll are 0.

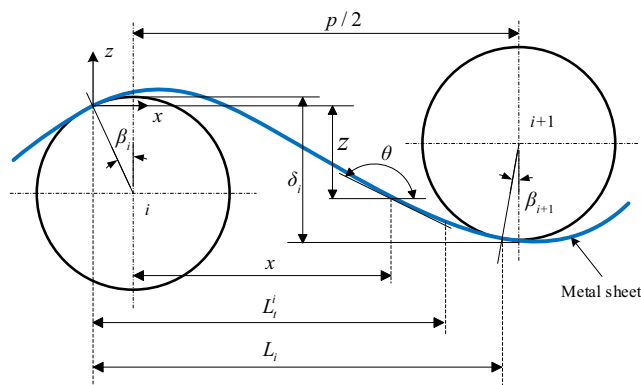
2.1 Geometric curvature integration model

The work rolls of the multi-roll leveller are numbered 1, 2, ..., n from the first roll at the entry to the last roll at the exit. A 2D geometric curvature integration model is established using the contact point of the sheet and the i th roll as the origin [7] as shown in Fig. 1.

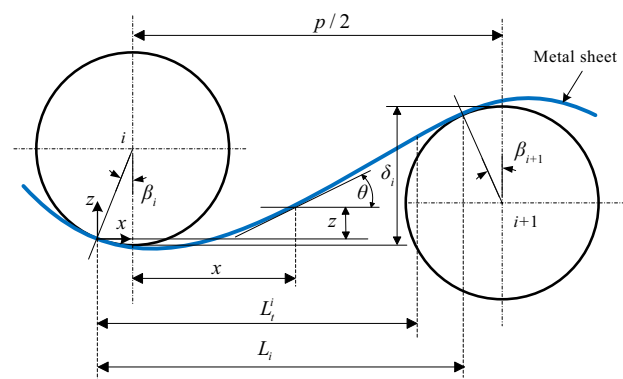
The contact points between the sheet and the work rolls are on the left side of the top and bottom points of the work rolls with contact angle β_i . The sheet between the two adjacent contact points gradually transitions from elastic deformation to elastoplastic deformation, wherein the total length of the section is L_i and the length of the elastic section is L_i^e . The tangent angle and radius of curvature of the sheet at any point (x, z) are θ and ρ , respectively. The intermesh value of the i th work roll is δ_i . Since the direction of the contact angle of the sheet and the work roll at the contact point are different for odd-numbered rolls and even-numbered rolls, it is necessary to establish two models.

A continuously differentiable curve can be described by Eq. (1):

$$\begin{cases} \rho \cdot d\theta \cdot \cos\theta = dx \\ dz = dx \cdot \tan\theta \end{cases} \quad (1)$$



(a) i is an odd-number



(b) i is an even-number

Fig. 1 Geometric curvature integration model. **a** i is an odd number. **b** i is an even number.

In levelling, the intermesh values of the work rolls are much smaller than the distance between the work rolls; therefore, $\theta \approx 0$. Based on this approximation, $\cos\theta \approx 1$ and $\tan\theta \approx \theta$. These approximations are substituted into Eq. (1) to obtain Eq. (2):

$$\begin{cases} \rho \cdot d\theta = dx \\ dz = \theta \cdot dx \end{cases} \quad (2)$$

As the basis of geometric curvature integration model, Eq. (2) is integrated over the interval 0 to x , and the radius of curvature ρ is replaced by the curvature A ($A = 1/\rho$); thus, Eq. (3) is obtained:

$$\begin{cases} \theta(x) = \int_0^x A(t) dt + C_1 \\ z(x) = \int_0^x \left(\int_0^q A(t) dt + C_1 \right) dq + C_2 \end{cases} \quad (3)$$

where t and q are integral variables, and C_1 and C_2 are integral constants.

When i is an odd number:

$$C_1 = \theta(x)|_{x=0} = \beta_i, \quad C_2 = z(x)|_{x=0} = 0.$$

When i is an even number:

$$C_1 = \theta(x)|_{x=0} = -\beta_i, \quad C_2 = z(x)|_{x=0} = 0.$$

The two equations above are uniformly expressed as Eq. (4):

$$C_1 = \theta(x)|_{x=0} = (-1)^{i+1} \beta_i, \quad C_2 = z(x)|_{x=0} = 0 \quad (4)$$

Equation (4) is substituted into Eqs. (3), and (5) is obtained:

$$\begin{cases} \theta(x) = \int_0^x A(t) dt + (-1)^{i+1} \beta_i \\ z(x) = \int_0^x \left(\int_0^q A(t) dt + (-1)^{i+1} \beta_i \right) dq \end{cases} \quad (5)$$

Equation (5) is integrated under the condition of $x = L_i$, and Eq. (6) is obtained:

$$\begin{cases} \theta(x)|_{x=L_i} = \int_0^{L_i} A(t) dt + (-1)^{i+1} \beta_i \\ z(x)|_{x=L_i} = \int_0^{L_i} \left(\int_0^q A(t) dt + (-1)^{i+1} \beta_i \right) dq \end{cases} \quad (6)$$

According to Fig. 1, the geometric constraint relationships shown in Eq. (7) is obtained:

$$\begin{cases} \theta(x)|_{x=L_i} = (-1)^i \beta_{i+1} \\ (-1)^i \cdot z(x)|_{x=L_i} + R(1 - \cos\beta_i) + R(1 - \cos\beta_{i+1}) = \delta_i \end{cases} \quad (7)$$

Equation (7) is substituted into Eqs. (6), and (8) is obtained:

$$\begin{cases} (-1)^i \beta_{i+1} = \int_0^{L_i} A(t) dt + (-1)^{i+1} \beta_i \\ \delta_i = (-1)^i \cdot \int_0^{L_i} \left(\int_0^q A(t) dt + (-1)^{i+1} \beta_i \right) dq + R(1 - \cos\beta_i) + R(1 - \cos\beta_{i+1}) \end{cases} \quad (8)$$

where

$$L_i = \frac{P}{2} + R\sin\beta_i - R\sin\beta_{i+1} \tag{9}$$

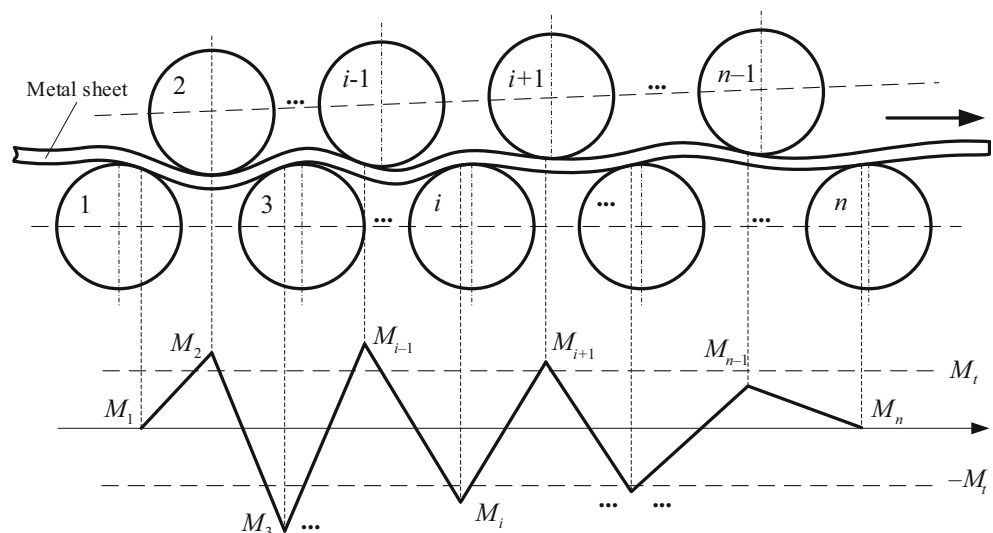
Equation (8) is a curvature-integrated geometric model established for a metal sheet between two adjacent work rolls. For a leveller with n work rolls, there are $n - 1$ equations similar to Eq. (8), and the total number of equations is $2(n - 1)$. The unknown parameters in Eq. (8) are the curvature $A(x)$ of the sheet, the corresponding integral term and the contact angle β_i of each work roll.

2.2 Bending-moment curvature model

The main forces applied to the sheet during levelling are the shearing forces of the work rolls, so the bending moment on the sheet is approximately linearly distributed between two adjacent contact points [6]. Therefore, the relationship between bending moment and curvature is established according to the material properties of the sheet and used to construct the bending-moment curvature model for multi-roll levelling. In this study, an ideal elastoplastic material is used to describe the metal sheet, regardless of the strengthening effect. This assumption is suitable for widely used low carbon steel.

Figure 2 shows the linear distribution of the bending moments on the sheet between the contact points in the leveller (assuming that the bending moment is positive when the sheet has a downward convex tendency in a purely curved state). From the entry to the exit of the leveller, the shearing forces applied by the work rolls on the sheet gradually decrease as the intermesh value of the work rolls decreases. The bending moment M_i at the contact point after the third roll exhibits a decreasing trend, and the bending moments of the first roll and the last roll are zero.

Fig. 2 Distribution of bending moments on the sheet cross-section in a multi-roll leveller



In the coordinate system shown in Fig. 1, the curvature and bending moment of the sheet at point x between the i th roll and the $i + 1$ th roll are $A(x)_i$ and $M(x)_i$, respectively. According to the linear distribution of bending moments shown in Fig. 2, $M(x)_i$ is

$$M(x)_i = \frac{M_{i+1} - M_i}{L_i} x + M_i \tag{10}$$

In the elastic section, the springback of the sheet after the reverse bending by the i th roll is completely elastic. According to the beam bending theory, if the curvature A of the sheet before bending is zero, then $1/\rho = M/EI$ in the elastic range. That is, $M = EIA$, where M is the bending moment of the cross section of the sheet, E is the elastic modulus of the sheet material, and I is the inertia moment of the cross section of the neutral layer of the sheet. However, the residual curvature A_c^i of the sheet after each springback in the multi-roll leveller has a non-negligible effect on the next reverse bending, so Eq. (10) is corrected to Eq. (11):

$$M(x)_i = EI(A(x)_i - A_c^i) \tag{11}$$

In Eq. (11), the influence of the residual curvature A_c^i after the reverse bending and the springback on the bending moment of the next reverse bending is taken into consideration. Therefore, the curvature coupling of the multi-roll levelling process is realized.

In the plastic section, according to the characteristics of the ideal elastoplastic material and considering the influence of residual curvature, the relationship between the bending moment and the curvature is derived as follows:

When i is an odd number:

$$M(x)_i = M_t \left[1.5 - 0.5 \frac{A_t^2}{(A(x)_i - A_c^i)^2} \right] \tag{12}$$

When i is an even number:

$$M(x)_i = -M_i \left[1.5 - 0.5 \frac{A_r^2}{(A(x)_i - A_c^i)^2} \right] \tag{13}$$

In Eqs. (12) and (13), A_r is the curvature at the elastic limit, which is the curvature of the sheet at the critical point between

elastic bending and elastoplastic bending, and M_i is the bending moment at the elastic limit.

Equation (14) is derived from Eqs. (10) and (13):

$$A(x)_i = \begin{cases} \frac{M_{i+1} - M_i}{EIL_i} x + \frac{M_i}{EI} + A_c^i & \text{(Elastic section : } (-1)^{i+1} M(x)_i \leq M_i) \\ (-1)^{i+1} \left(\frac{M_i A_r^2}{3M_i + 2(-1)^i M_i + 2(-1)^i \frac{M_{i+1} - M_i}{L_i} x} \right)^{\frac{1}{2}} + A_c^i & \text{(Elastoplastic section : } (-1)^{i+1} M(x)_i > M_i) \end{cases} \tag{14}$$

The moment curvature model shown in Eq. (14) contains the residual curvature term A_c^i . This model describes the curvature of the sheet in the elastic section and the elastoplastic section and identifies the location on the sheet where the bending moment exceeds M_i .

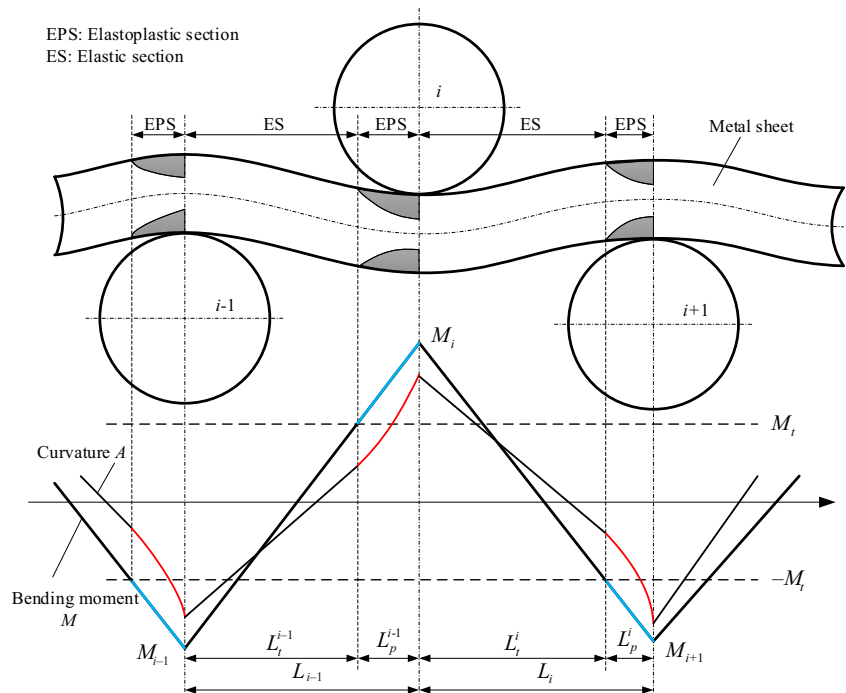
According to Eq. (14), Fig. 3 demonstrates the distribution of the elastic and elastoplastic sections of the sheet during the reverse bending process and illustrates the variation of the bending moment and curvature in the two sections. The elastoplastic section is only a small section before the point of contact between the sheet and the work roll, and the rest of the sheet is part of the elastic section. The bending moment varies linearly in the whole section; the curvature varies linearly in the

elastic section and nonlinearly in the elastoplastic section.

3 Solution and verification of the coupled curvature integration model

The coupled curvature integration model for multi-roll leveling consists of the geometric model (Eq. (8)) and the bending-moment curvature model (Eq. (14)). The former describes the relationship between the intermesh values and the curvature, and the latter describes the relationship between the bending moment and the curvature. There are three major difficulties preventing a direct solution of the coupled curvature

Fig. 3 Distribution of the elastic section and elastoplastic sections of the sheet



integration model, as follows: first, the equations contain definite integral terms of unknown variables; second, the equations are highly nonlinear and contain many unknown variables; and third, the curvature $A(x)_i$ in the equations is an unknown variable expressed by a piecewise function that depends on another unknown variable $M(x)_i$.

3.1 Solution of the model

To easily convert the integral term in Eq. (8), let

$$\begin{cases} a_i = (-1)^{i+1} \\ b_i = \frac{M_t A_t^2 L_i}{2(-1)^i (M_{i+1} - M_i)} \\ c_i = \frac{(3M_t + 2(-1)^i M_i) L_i}{2(-1)^i (M_{i+1} - M_i)} \\ d_i = \frac{M_{i+1} - M_i}{E I L_i} \\ e_i = \frac{M_i}{E I} \end{cases} \quad (15)$$

For a leveller with n work rolls, i takes values from 0 to $n - 1$ in Eq. (15).

Equation (15) is substituted into Eqs. (14), and (16) is obtained after simplification:

$$A(x)_i = \begin{cases} d_i x + e_i + A_c^i & \text{(Elastic section : } (-1)^{i+1} M(x)_i \leq M_t) \\ a_i \left(\frac{b_i}{x + c_i} \right)^{\frac{1}{2}} + A_c^i & \text{(Elastoplastic section : } (-1)^{i+1} M(x)_i > M_t) \end{cases} \quad (16)$$

Equation (16) is substituted into the first equation given in q. (8), and the following equation is obtained:

$$-a_i \beta_{i+1} = \int_0^{L_i} (d_i \cdot t + e_i + A_c^i) dt + \int_{L_i}^{L_i} \left(a_i \left(\frac{b_i}{t + c_i} \right)^{\frac{1}{2}} + A_c^i \right) dt + a_i \beta_i$$

The above equation is solved using the definite integral. After rearranging the terms, Eq. (17) is obtained:

$$a_i (\beta_i + \beta_{i+1}) + L_i^i \left(A_c^i + e_i + \frac{1}{2} d_i L_i^i \right) + \left(2a_i b_i^{\frac{1}{2}} \left((L_i + c_i)^{\frac{1}{2}} - (L_i^i + c_i)^{\frac{1}{2}} \right) + A_c^i (L_i - L_i^i) \right) = 0 \quad (17)$$

Equation (17) converts the first equation given in Eq. (8) from an integral equation to an algebraic equation.

Let y_i be the integral term in the second equation given in Eq. (8), i.e.

$$y_i = \int_0^{L_i} \left(\int_0^q A(t) dt + (-1)^{i+1} \beta_i \right) dq \quad (18)$$

Equation (16) is substituted into Eq. (18), and the following equation is obtained:

$$y_i = \int_0^{L_i} \left(\int_0^q (d_i \cdot t + e_i + A_c^i) dt + a_i \beta_i \right) dq + \int_{L_i}^{L_i} \left(\int_0^{L_i} (d_i \cdot t + e_i + A_c^i) dt + \int_{L_i}^q \left(a_i \left(\frac{b_i}{x + c_i} \right)^{\frac{1}{2}} + A_c^i \right) dt + a_i \beta_i \right) dq$$

Let

$$y_i = u_i + v_i \quad (19)$$

where

$$\begin{cases} u_i = \int_0^{L_i} \left(\int_0^q (d_i \cdot t + e_i + A_c^i) dt + a_i \beta_i \right) dq \\ v_i = \int_{L_i}^{L_i} \left(\int_0^{L_i} (d_i \cdot t + e_i + A_c^i) dt + \int_{L_i}^q \left(a_i \left(\frac{b_i}{x + c_i} \right)^{\frac{1}{2}} + A_c^i \right) dt + a_i \beta_i \right) dq \end{cases}$$

u_i and v_i are solved separately as shown in Eqs. (20), and (21) is obtained:

$$\begin{aligned} u_i &= \int_0^{L_i} \left(\int_0^q (d_i \cdot t + e_i + A_c^i) dt + a_i \beta_i \right) dq \\ &= \int_0^{L_i} \left(\frac{1}{2} d_i q^2 + (e_i + A_c^i) q + a_i \beta_i \right) dq \\ &= \frac{1}{6} d_i (L_i^i)^3 + \frac{1}{2} (e_i + A_c^i) (L_i^i)^2 + a_i \beta_i L_i^i \end{aligned} \quad (20)$$

$$\begin{aligned}
v_i &= \int_{L_i^i}^{L_i^i} \left(\int_0^{L_i^i} (d_i \cdot t + e_i + A_c^i) dt + \int_{L_i^i}^q \left(a_i \left(\frac{b_i}{x + c_i} \right)^{\frac{1}{2}} + A_c^i \right) dt + a_i \beta_i \right) dq \\
&= \int_{L_i^i}^{L_i^i} \left(\left(\frac{1}{2} d_i (L_i^i)^2 + (e_i + A_c^i) L_i^i \right) + 2a_i b_i^{\frac{1}{2}} \left((q + c_i)^{\frac{1}{2}} - (L_i^i + c_i)^{\frac{1}{2}} \right) + A_c^i (q - L_i^i) + a_i \beta_i \right) dq \\
&= \int_{L_i^i}^{L_i^i} \left(\left(\frac{1}{2} d_i (L_i^i)^2 + e_i L_i^i - 2a_i b_i^{\frac{1}{2}} (L_i^i + c_i)^{\frac{1}{2}} + a_i \beta_i \right) + 2a_i b_i^{\frac{1}{2}} (q + c_i)^{\frac{1}{2}} + A_c^i q \right) dq \\
&= \left(\frac{1}{2} d_i (L_i^i)^2 + e_i L_i^i - 2a_i b_i^{\frac{1}{2}} (L_i^i + c_i)^{\frac{1}{2}} + a_i \beta_i \right) (L_i - L_i^i) + 2a_i b_i^{\frac{1}{2}} \left(\frac{2}{3} (L_i + c_i)^{\frac{3}{2}} - \frac{2}{3} (L_i^i + c_i)^{\frac{3}{2}} \right) \\
&\quad + \frac{1}{2} A_c^i (L_i^2 - (L_i^i)^2)
\end{aligned} \tag{21}$$

Equations (18) and (19) are substituted into the second equation given in Eqs. (8), and (22) is obtained:

$$\delta_i + a(u_i + v_i) - R(1 - \cos \beta_i) - R(1 - \cos \beta_{i+1}) = 0 \tag{22}$$

Equation (22) represents the conversion of the second equation given in Eq. (8) from an integral equation to an algebraic equation.

Therefore, Eq. (8) is transformed into the algebraic form shown in Eq. (23):

$$\begin{cases} a_i(\beta_i + \beta_{i+1}) + L_i^i \left(A_c^i + e_i + \frac{1}{2} d_i L_i^i \right) + \left(2a_i b_i^{\frac{1}{2}} \left((L_i + c_i)^{\frac{1}{2}} - (L_i^i + c_i)^{\frac{1}{2}} \right) + A_c^i (L_i - L_i^i) \right) = 0 \\ \delta_i + a_i(u_i + v_i) - R(1 - \cos \beta_i) - R(1 - \cos \beta_{i+1}) = 0 \end{cases} \tag{23}$$

Equation (23) consists of $2n - 2$ equations ($n - 1$ pairs); the equations contain $2n - 2$ basic unknowns (n contact angles from β_1 to β_n , and $n - 2$ bending moments from M_2 to M_{n-1}) and some auxiliary unknowns, so the equations are solvable. It is necessary to establish the relationships between the basic unknowns and the auxiliary unknowns to solve the equations, so the undetermined variables L_i^i and A_c^i will be discussed below.

As shown in Figs. 1 and 3, the length of the elastic section of the sheet is L_i^i , which is defined by the elastic limit bending moment M_i as boundary point. In the interval of the sheet from the i th roll to the $i + 1$ th roll, the following relationships can be defined: if $M_{i+1} > M_i$, then $L_i^i < L_i$, and if $M_{i+1} < M_i$, then $L_i^i = L_i$. Therefore, Eq. (24) can be derived:

$$L_i^i = \begin{cases} \frac{(-1)^{i+1} M_i - M_i}{M_{i+1} - M_i} L_i & \left((-1)^{i+1} M_{i+1} \leq M_i \right) \\ L_i & \left((-1)^{i+1} M_{i+1} > M_i \right) \end{cases} \tag{24}$$

The recursive method is used to calculate A_c^i . Plastic deformation will occur in the interval of the sheet from the i th roll to the $i + 1$ th roll if M_{i+1} is greater than M_i . $x = L_i$ is substituted

into Eqs. (14), and (25) is obtained:

$$A_{i+1}^i = \begin{cases} \frac{M_{i+1}}{EI} + A_c^i & \left((-1)^{i+1} M_{i+1} \leq M_i \right) \\ (-1)^{i+1} \left(\frac{M_i A_i^2}{3M_i - 2M_{i+1}} \right)^{\frac{1}{2}} + A_c^i & \left((-1)^{i+1} M_{i+1} > M_i \right) \end{cases} \tag{25}$$

Equation (26) is known:

$$A_c^{i+1} = A_{i+1}^i - \frac{M_{i+1}}{EI} \tag{26}$$

Since M_1 is zero, Eq. (27) is obtained:

$$A_c^1 = A_0 \tag{27}$$

Based on Eqs. (25), (26) and (27), Eq. (28) is obtained:

$$\begin{cases} A_c^{i+1} = \begin{cases} A_c^i & \left((-1)^{i+1} M_{i+1} \leq M_i \right) \\ (-1)^{i+1} \left(\frac{M_i A_i^2}{3M_i - 2M_{i+1}} \right)^{\frac{1}{2}} - \frac{M_{i+1}}{EI} + A_c^i & \left((-1)^{i+1} M_{i+1} > M_i \right) \end{cases} \\ A_c^1 = A_0 \end{cases} \tag{28}$$

Equation (28) shows the recursive relationship of A_c^i and the known initial value A_0 , so it is possible to solve for A_c^i . For a leveller with n work rolls, the subscripts i of the intermediate variables $a_i, b_i, c_i, d_i, e_i, L_i^i$ and L_i range from 1 to $n - 1$. The subscripts i of A_c^i and A_i range from 1 to n .

In summary, a set of nonlinear equations for the coupled curvature integration model in multi-roll levelling process can be built by the flow diagram in Fig. 4. First, a geometric model established for a metal sheet between the two adjacent work rolls can be obtain in Eq. (8). Then, considering the influence of the residual curvature on the next reverse bending, $M(x)$, is changed in Eq. (10). Also, the intervals in the definite integrals are divided into the elastic and elastoplastic sections (Eq. 24). By calculating the definite integrals respectively, Eq. (8) can be transformed into the algebraic equation. The step of building Eq. (23) will continue until $i = n - 1$. Finally, the nonlinear

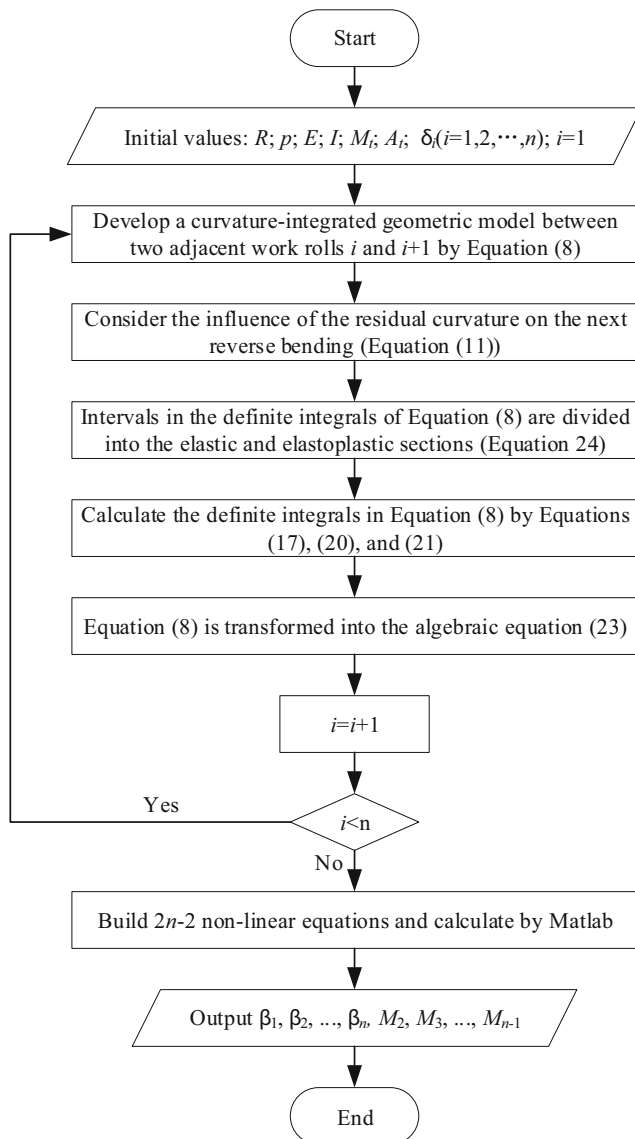


Fig. 4 Flow diagram of building the coupled curvature integration model

Table 1 The experimental levelling parameters of the metal sheet

Parameters	Values
Number of work rolls	10
Diameter of work rolls (mm)	40
Distance between work rolls (mm)	42
Yield stress of the metal sheet (MPa)	180
Elastic modulus of the metal sheet (GPa)	210
Thickness of the metal sheet (mm)	0.8
Entry intermesh value (mm)	1.20
Exit intermesh value (mm)	-0.2

equations are assembled and calculated by Matlab. The $2n - 2$ equations have $2n - 2$ basic unknowns, including n contact angles ranging from β_1 to β_n and $n - 2$ bending moments ranging from M_2 to M_{n-1} .

3.2 Verification of the model

The results calculated by the coupled curvature integration model are based on the experimental data by Soda. The experimental levelling parameters of the metal sheet are listed in Table 1.

Figure 5 demonstrates the curvature of the sheet at the points of contact with each work roll. Compared with other calculated results [7, 39, 40], The coupled curvature integration model studied in this paper is more consistent with the experimental results than the other models, especially the curvature in the last work roll.

4 Analysis of the key parameters in multi-roll levelling

The effect of levelling on longitudinal waves is gauged by the residual curvature A_c^e after levelling, that is, the curvature of

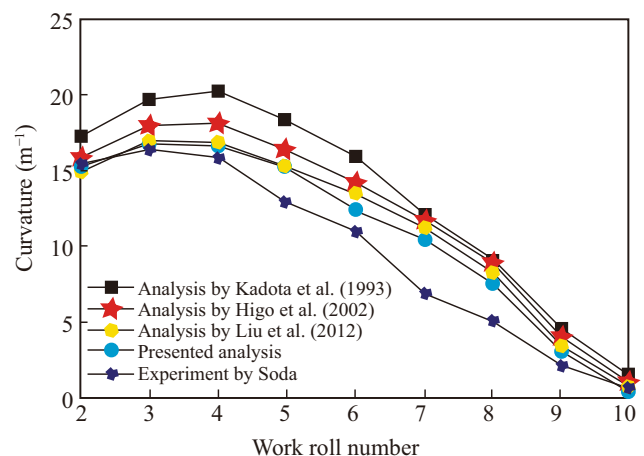


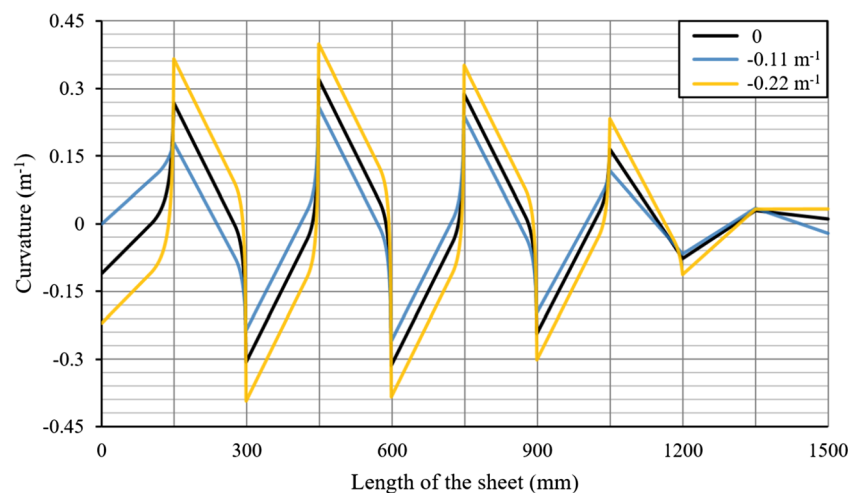
Fig. 5 Comparison of curvatures at the work rolls

Table 2 Multi-roll levelling parameters

Parameters	Values
Number of work rolls	11
Diameter of work rolls (mm)	280
Distance between work rolls (mm)	300
Yield stress of the metal sheet (MPa)	127.6
Elastic modulus of the metal sheet (GPa)	115.9
Thickness of the metal sheet (mm)	20
Width of the metal sheet (mm)	3000

the sheet as it leaves the last work roll. To obtain a smaller residual curvature A_c^g , it is necessary to investigate the variation of the sheet inside the leveller. Key parameters, such as curvature, surface profile curve and the plastic deformation rate of the sheet, describe the levelling process in terms of the variation of bending characteristics, shape evolution and elastoplastic deformation. Studying the dynamic changes in these parameters is helpful for achieving better levelling results. The levelling parameters are listed in Table 2, and the intermesh values and initial curvatures are specified in the discussion.

Figure 6 depicts the curvature variation of the sheets during the multi-roll levelling using three different initial curvatures. The straight and curved sections of the lines represent the elastic and elastoplastic sections of the sheets, respectively. The elastoplastic sections are shorter than the elastic sections, but the curvature of the former varies drastically. The initial curvature difference between the three sheets is in increments of 0.11 m^{-1} , and the difference between the sheets after levelling is less than 0.02 m^{-1} . The results show that the multi-roll levelling can gradually reduce the curvatures of the sheets. The levelling process is consistent, and curvatures approaching zero are possible.

Fig. 6 Curvature distribution of the sheets in levelling

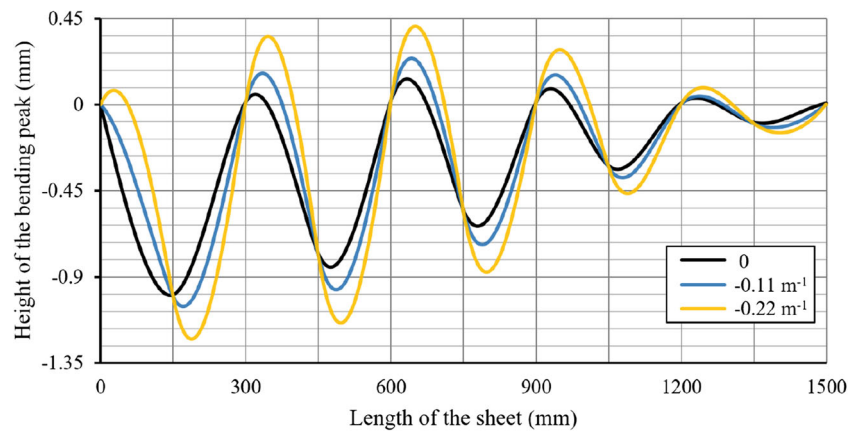
The macro levelling effect of the longitudinal waves can be described by the surface profile curve of the sheet. Figure 7 shows the surface profile curves of the three sheets with different levelling curvatures. The three sheets exhibit characteristics of alternating reverse bending under the action of the upper and lower work rolls, and the bending peak is gradually reduced, eventually approaching zero. As the initial curvature of the sheets increases from 0 to 0.22 m^{-1} , the peak value of the curve increases, the spacing between the peaks decreases, and the levelling difficulty increases.

The plastic deformation rate is the ratio of the thickness of the plastic deformation section to the original thickness of the sheet. This ratio has a significant influence in eliminating the initial residual stress because the residual stress of the sheet only changes in the plastic deformation section, i.e. it does not change in the elastic deformation section. Figure 8 shows the plastic deformation rate of the three sheets with different initial curvatures at the contact points of the work rolls. The larger the initial curvature is, the greater the plastic deformation rate of the levelling. The bending moments of the sheets at the first and last work rolls are zero, and the plastic deformation rates are zero.

5 Influence of the intermesh on the levelling effect

The intermesh value is an important parameter in the levelling process. This value directly influences the levelling effect, that is, the value of the residual curvature. There are two main issues that need to be addressed: The first issue is how to adjust the entry intermesh value δ_e and the exit intermesh value δ_g so that the residual curvature A_c^g of the processed sheet is as

Fig. 7 Surface profile curves in levelling



close as possible to zero. The second issue is how to control the sensitivity of the residual curvature A_c^g to a level within the adjustment error of the intermesh value to ensure the stability of the levelling effect.

First, the method of making the residual curvature A_c^g as close as possible to zero is investigated. Figure 9 demonstrates the residual curvature of a sheet with an initial curvature of -0.11 m^{-1} after levelling. The residual curvature is calculated using a coupled curvature integration model with entry intermesh values ranging from 0.5 to 1.4 mm and exit intermesh values ranging from -0.3 to 0.3 mm. The distribution of residual curvature is similar to a wave as shown in Fig. 9. Due to the wave-like distribution of the residual curvature, there are many exit intermesh values that can make the residual curvature approach zero for a given entry intermesh value. Alternatively, there are also many entry intermesh value that can make the residual curvature approach zero for a given exit intermesh value. As the entry intermesh value and the exit intermesh value increase, the residual curvature also shows an increasing trend, and the levelling effect deteriorates.

Figure 10 demonstrates the intersection of a plane with zero residual curvature and the residual curvature

surface. The intersection lines indicate intermesh values that produce a residual sheet curvature of zero; theoretically, this set of values is infinite.

Second, the sensitivity of the residual curvature to variations of the entry intermesh value and the exit intermesh value is investigated. Figure 11 demonstrates the variation of the residual curvature as a function of the exit intermesh value δ_g for four different entry intermesh values δ_e of 0.7 mm, 0.9 mm, 1.1 mm and 1.3 mm. The four curves are close to sinusoidal. As the entry intermesh value increases, the peak value of the curve increases significantly; thus, the slope of the curve near zero also increases significantly, so the sensitivity of the residual curvature increases. Therefore, an error in the exit intermesh value will cause the residual curvature to fluctuate within a large range.

6 Conclusions

The present residual stress analysis models have not fully addressed the curvature coupling of repeated sheet bending. To address this problem, this work analysed the multi-roll levelling of longitudinal waves that is achieved by a repeated and gradual decrease of elastoplastic bending deformation. The work also established a coupled curvature integration model that combines geometric coupling and curvature coupling. Compared with the experimental data presented in the references, the proposed model is more accurate. The variation of the curvature, the surface profile curve and the plastic deformation rate of the sheet in a leveler were analysed using the model. Two criteria were proposed to evaluate the levelling of longitudinal waves, as follows: the residual curvature after levelling and the sensitivity of the residual curvature to the intermesh value. The influence of the work roll intermesh value

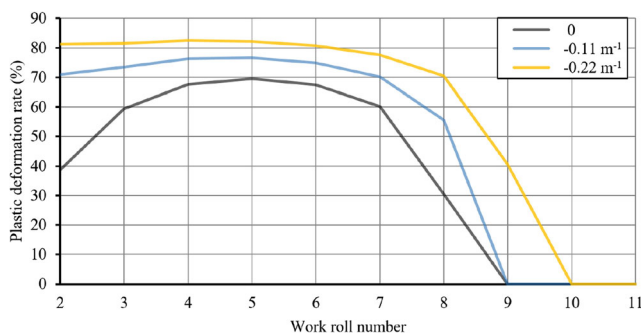


Fig. 8 Plastic deformation rate of the sheets in levelling

Fig. 9 Relationship between residual curvature and intermesh value

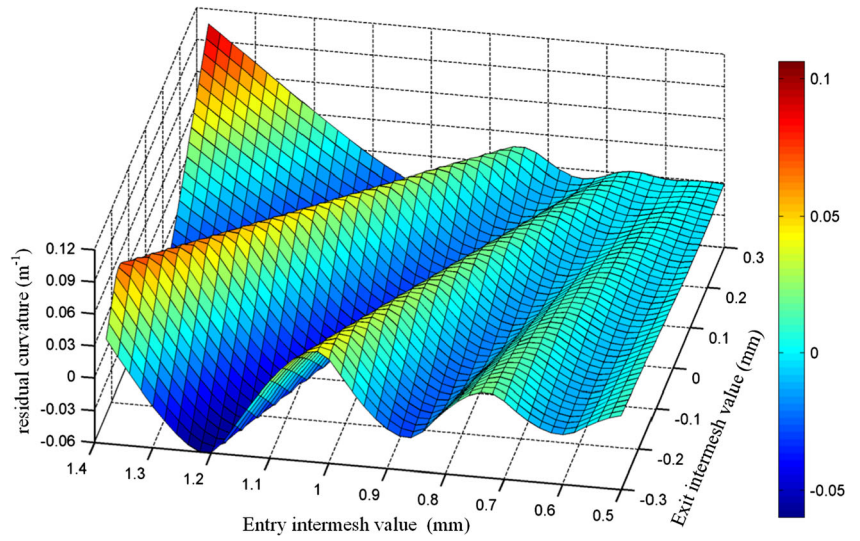


Fig. 10 Intermesh value corresponding to zero residual curvature

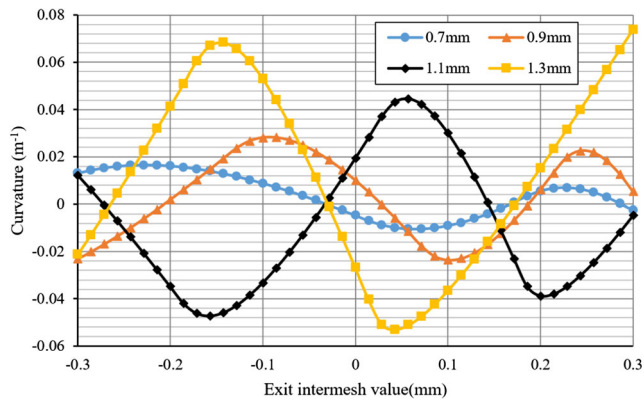
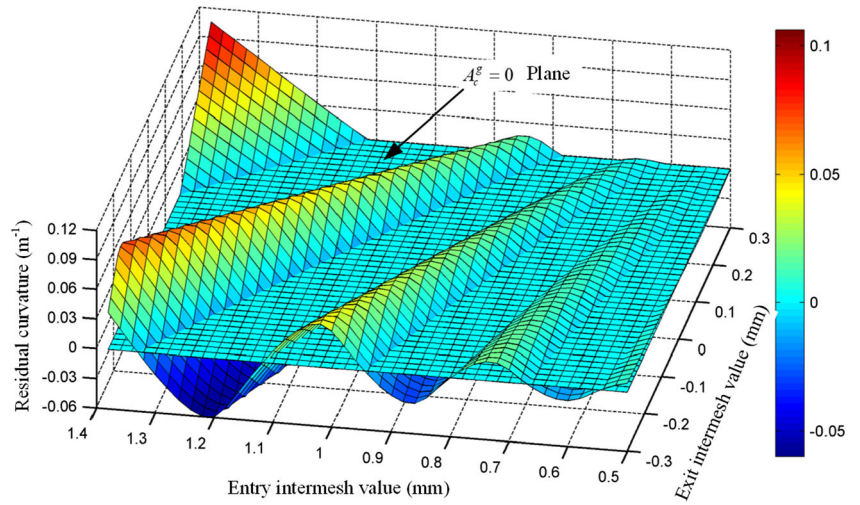


Fig. 11 Relationship between residual curvature and the exit intermesh value

on the levelling effect was studied, and the following conclusions were drawn: First, for a given sheet, there are infinite combinations of entry intermesh values and exit intermesh values that make the residual curvature zero. Second, the variation of the entry intermesh value has a significant effect on the sensitivity of the residual curvature relative to the exit intermesh value.

Funding information The authors would like to thank the National Key R&D Program of China (Grant No. 2018YFB1701601) and the National Natural Science Foundation of China (Grant No. 51875515) for the support given to this research.

References

- Fischer FD, Rammerstorfer FG, Friedl N, Wieser W (2000) Buckling phenomena related to rolling and levelling of sheet metal. *Int J Mech Sci* 42(10):1887–1910
- Abdelkhalek S, Montmitonnet P, Legrand N, Buessler P (2008) Manifested flatness predictions in thin strip cold rolling. *Int J Mater Form* 1(1):339–342
- Weiss M, Abeyathna B, Rolfe B, Abee A, Wolfkamp H (2017) Effect of coil set on shape defects in roll forming steel strip. *J Manuf Process* 25:8–15
- Woo YY, Han SW, Hwang TW, Park JY, Moon YH (2018) Characterization of the longitudinal bow during flexible roll forming of steel sheets. *J Mater Process Technol* 252:782–794
- Nakhoul R, Montmitonnet P, Potier-Ferry M (2015) Multi-scale method for modeling thin sheet buckling under residual stresses in the context of strip rolling. *Int J Solids Struct* 66:62–76
- Doege E, Menz R, Huinink S (2002) Analysis of the levelling process based upon an analytic forming model. *Cirp Ann-Manuf Technol* 51(1):191–194
- Liu ZF, Wang YQ, Yan XC (2012) A new model for the plate leveling process based on curvature integration method. *Int J Mech Sci* 54(1):213–224
- Tran DC, Tardif N, Limam A (2015) Experimental and numerical modeling of flatness defects in strip cold rolling. *Int J Solids Struct* 69–70:343–349
- Abvabi A, Rolfe B, Hodgson PD, Weiss M (2016) An inverse routine to predict residual stress in sheet material. *Mater Sci Eng A* 652:99–104
- Yu G, Zhai R, Zhao J, Ma R (2018) Theoretical analysis and numerical simulation on the process mechanism of two-roller straightening. *Int J Adv Manuf Technol* 94:4011–4021
- Wang Y, Zhu XQ, Wang Q, Cui XM (2019) Research on multi-roll roll forming process of thick plate. *Int J Adv Manuf Technol* 102(1–4):17–26
- Tran DC, Tardif N, El Khaloui H, Limam A (2017) Thermal buckling of thin sheet related to cold rolling: latent flatness defects modeling. *Thin-Walled Struct* 113:129–135
- Grüber M, Hirt G (2018) Investigation of correlation between material properties, process parameters and residual stresses in roller levelling. *Proc Manuf* 15:844–851
- Silvestre E, de Argandona ES, Galdos L, Mendiguren J (2014) Testing and modeling of roll levelling process. *Key Eng Mater* 611–612:1753–1762
- Behrens BA, El Nadi T, Krimm R (2011) Development of an analytical 3D-simulation model of the levelling process. *J Mater Process Technol* 211(6):1060–1068
- Chen WH, Liu J, Cui ZS, Wang YJ, Wang YR (2015) A 2.5-dimensional analytical model of cold leveling for plates with transverse wave defects. *J Iron Steel Res Int* 22(8):664–671
- Brauneis R, Steinboeck A, Jochum M, Kugi A (2018) A robust real-time model for plate leveling. *Ifac Papersonline* 51(2):61–66
- Feng X, Montmitonnet P, Yang Q, He A, Wang X (2017) An advanced 3D mathematical model for a 6-high tandem cold rolling process. *Proc Eng* 207:1379–1384
- Abdelkhalek S, Montmitonnet P, Potier-Ferry M, Zahrouni H, Legrand N, Buessler P (2010) Strip flatness modelling including buckling phenomena during thin strip cold rolling. *Ironmak Steelmak* 37(4):290–297
- Weiss M, Rolfe B, Hodgson PD, Yang CH (2012) Effect of residual stress on the bending of aluminium. *J Mater Process Technol* 212(4):877–883
- Traub T, Chen X, Groche P (2017) Experimental and numerical investigation of the bending zone in roll forming. *Int J Mech Sci* 131:956–970
- Mathieu N, Potier-Ferry M, Zahrouni H (2017) Reduction of flatness defects in thin metal sheets by a pure tension leveler. *Int J Mech Sci* 122:267–276
- Stadler G, Steinboeck A, Kugi A (2017) Control of curvature and contact force of a metal strip at the strip-roll contact point. *Ifac Papersonline* 50(1):11325–11330
- Lu HS, Cheng HS, Cao J, Liu WK (2005) Adaptive enrichment meshfree simulation and experiment on buckling and post-buckling analysis in sheet metal forming. *Comput Methods Appl Mech Eng* 194(21–24):2569–2590
- Liu ZF, Wang YQ, Ou HG, Yan XC, Luo YX (2014) An analytical leveling model of curvature and residual stress simulation for H-beams. *J Constr Steel Res* 102:13–23
- Tsang KS, Ion W, Blackwell P, English M (2017) Validation of a finite element model of the cold roll forming process on the basis of 3D geometric accuracy. *Proc Eng* 207:1278–1283
- Abdelkhalek S, Montmitonnet P, Legrand N, Buessler P (2011) Coupled approach for flatness prediction in cold rolling of thin strip. *Int J Mech Sci* 53(9):661–675
- Dratz B, Nalewajk V, Bikard J, Chastel Y (2009) Testing and modelling the behaviour of steel sheets for roll levelling applications. *Int J Mater Form* 2(1):519–522
- Lee CW, Yang DY, Kang DW, Lee TW (2014) Study on the leveling process of the current collector for the molten carbonate fuel cell based on curvature integration method. *Int J Hydrog Energy* 39(12):6714–6728
- Nakhoul R, Montmitonnet P, Legrand N (2015) Manifested flatness defect prediction in cold rolling of thin strips. *Int J Mater Form* 8(2):283–292
- Galkina A, Gafur I, Schlacher K (2017) Model predictive control with linear programming for the strip Infeed in hot rolling mills. *Ifac Papersonline* 50(1):11301–11306
- Laugwitz M, Seuren S, Jochum M, Hojda S, Lohmar J, Hirt G (2017) Development of levelling strategies for heavy plates via controlled FE models. *Proc Eng* 207:1349–1354
- Baumgart M, Steinboeck A, Kugi A, Raffin-Peyloz G, Irastorza L, Kiefer T (2012) Optimal active deflection compensation of a hot leveler. *IFAC Proc* 45(23):30–35
- Nakhoul R, Montmitonnet P, Abdelkhalek S (2012) Flatness defect in thin strip cold rolling and the friction impact on it. *Trans N Am Manuf Res Instit SME* 40:277–286
- Liu ZF, Luo YX, Yan XC, Wang YQ (2015) Boundary determination of leveling capacity for plate roller leveler based on curvature integration method. *J Cent South Univ* 22(12):4608–4615
- Brauneis R, Baumgart M, Steinboeck A, Kugi A, Jochum M (2017) Deflection model of a multi-actuator gap leveler. *Ifac Papersonline* 50(1):11295–11300
- Cui L, Hui XL, Liu XH (2011) Analysis of leveling strategy for a plate mill. *Adv Mater Res-Switz* 145:424–428

38. Cui L, Shi QQ, Liu XH, Hu XL (2013) Residual curvature of longitudinal profile plate roller in leveling process. *J Iron Steel Res Int* 20(10):23–27
39. Kadota K, Maeda R (1993) A model of analysis of curvature in leveling process - numeric study of roller leveling process. 34:481
40. Higo T, Matsumoto H, Ogawa S (2012) Effects of numerical expression of stress-strain curve on curvature of material of roller leveling process. *J Japan Soc Technol Plast* 43(496):439–443

Publisher's note Springer Nature remains neutral with regard to jurisdictional claims in published maps and institutional affiliations.